Enhancement of conductance fluctuations in a mesoscopic system of strong scatterers

V. V. Marinyuk[1] and D. B. Rogozkin[1,2]

[1]*Moscow Engineering Physics Institute (National Research Nuclear University), Kashirskoe Shosse 31, 115409 Moscow, Russia*

[2]*N.L. Dukhov All-Russia Research Institute of Automatics, Sushchevskaya Street 22, 127055 Moscow, Russia*

(Received 23 January 2017; revised manuscript received 28 September 2017; published 30 October 2017)

We study how the conductance fluctuations change in a disordered ensemble of strongly scattering (non-Born) centers. Diagrammatic calculations of the conductance variance are carried out beyond the standard Born definition for the Hikami vertex. For a system of strong pointlike scatterers, the enhancement of the conductance fluctuations is found in the crossover between ballistic and diffusive regimes. The incoherent contribution arising from random spatial variations in the scatterer concentration is primarily responsible for the enhancement of fluctuations. In the limit of resonant scatterers, the coherent contribution to the conductance variance also peaks in the crossover regime and its maximum exceeds the UCF value.

DOI: 10.1103/PhysRevB.96.155146

I. INTRODUCTION

The phase-coherent transport through disordered systems has motivated a rather intensive research activity for three decades. The subject is common to several areas of physics ranging from solid state and mesoscopic physics to classical wave scattering. Different phenomena in quantum electron transport and in propagation of electromagnetic waves are closely connected by underlying chaotic dynamics and subject to universal statistical laws [1].

Mesoscopic conductance fluctuations represent one of the most famous manifestations of phase-coherent transport in electron conductors (quantum wires, dots, etc.) [2–8] and disordered waveguides [9–12]. Much previous work has been focused on the universal statistical properties which are inherent to the diffusive regime of wave propagation, where the effect of the universal conductance fluctuations (UCF) is observed (see, e.g., [1–5,9,13,14]). Due to the coherence of the wave motion over the entire sample, the variance of dimensionless conductance is of order unity, with no dependence on the system size and the scattering properties.

There are also a number of studies where the crossover from the ballistic to diffusive transport was investigated [15–23]. The results [15–23] suggest an enhancement of fluctuations at subdiffusion scales. Specifically, the conductance variance can exceed the value that is achieved in the diffusive regime (i.e., the UCF value). Of particular interest is to clarify the conceivable reasons for such behavior of conductance fluctuations and its correlation with the specific features of disorder. Small-angle scattering [24] by large-scale inhomogeneities is one reason [23,25–27]. The other reason can be associated with strong individual scatterers [28]. The latter case is studied below.

We consider the mesoscopic conductance fluctuations in a disordered system of strong scatterers. Going beyond the Born approximation, we take simultaneously into account both random interference of waves and the effect from random local deviations of the scatterer concentration from its average value. As has been suggested previously [24,29–33], both these mechanisms can cause conductance fluctuations.

The interference mechanism dominates provided that the coherence length is much greater than the elastic mean free path (the "universal" conductance fluctuations is observed where the coherence length exceeds the sample size). This mechanism, as applied to electron transport, dominates at low temperatures. The conductance fluctuations due to local variations in scattering properties (see, e.g., [24,29–31]) are believed to prevail at relatively high temperatures. Although both mechanisms act simultaneously, they have never been considered within any unified theoretical treatment. Up to now the contribution of the second mechanism of fluctuations to the conductance variance was estimated only within a number of particular models oriented to the specific conditions of electron scattering in solids [29–33] and also in the weak scattering limit [24].

For classical waves (light, microwaves) there are no restrictions that are inherent to electron transport (e.g., the decrease in the phase coherence length with increasing temperature), and both mechanisms of conductance fluctuations should equally be taken into account.

In this paper we present a novel result for the variance of sample-to-sample conductance fluctuations in a quasi-one-dimensional (1D) system (a waveguide with bulk disorder). The diagrammatic calculations are carried out beyond the standard Born definition for the Hikami vertex. The variance is expressed explicitly in terms of the amplitude of scattering by a single center and the propagators that obey the conventional transport equation. Allowance for all necessary correlations between wave fields (not only the pair correlations) enables us to include the effect of random variations in the scatterer concentration. This leads to the appearance of an incoherent contribution (having noninterference origin) to the conductance variance. The coherent contribution also changes as compared to the result obtained previously [23]. For a system of pointlike centers, the obtained analytical expression for the conductance variance extends the well-known random matrix theory (RMT) result [34,35] to the case of strong single-center scattering. We show that the conductance variance reaches its maximum in the crossover between the quasiballistic and diffusive regimes, and tends to the UCF value in the large-length limit.

II. SEMICLASSICAL ANALYSIS

Consider transmission of monochromatic waves through a disordered waveguide of length L. The dimensionless conductance (or transmittance) of the waveguide can be

defined as the sum of transmission coefficients T_{ab} connecting incoming and outgoing modes a and b, respectively (see, e.g., [1,14]):

$$G = \sum_{a,b} T_{ab}. \tag{1}$$

The transmission coefficients T_{ab} depend on spatial configuration of the scattering centers and vary from sample to sample.

To give insight into the physical origin of mesoscopic conductance fluctuations, we first consider this phenomenon qualitatively within semiclassical analysis of wave transport in a disordered system.

The transmission coefficient T_{ab} entering into Eq. (1) can be expressed in terms of the square of the sum over all paths of the semiclassical amplitude to transit from incoming mode a at the input boundary to outgoing mode b at the output one. The amplitude is proportional to the product of a set of the Green functions which describe the sequence of scattering events along a given path [4]. This gives

$$T_{ab} = \left| \sum_i A_i^{ab} \right|^2 = \sum_i \left| A_i^{ab} \right|^2 + \sum_{i \neq j} A_i^{ab} A_j^{ab*}, \tag{2}$$

where the summation over all paths i is carried out. The first term is the sum of classical transition probabilities and is responsible for ray- or particlelike transport through the sample. The second term describes interference of the waves propagating along differing paths.

Only the first term of Eq. (2) makes a contribution to the disorder-averaged conductance $\langle G \rangle$. The "interference" term appearing in Eq. (2) fluctuates with changes in configuration of scattering centers because of the difference in phases between the waves propagating along differing paths, and vanishes when averaged over disorder.

The variance of conductance fluctuations can be written as

$$\langle (\delta G)^2 \rangle = \sum_{abcd} \left(\left\langle \sum_i \left| A_i^{ab} \right|^2 \sum_j \left| A_i^{cd} \right|^2 \right\rangle - \left\langle \sum_i \left| A_i^{ab} \right|^2 \right\rangle \left\langle \sum_j \left| A_j^{cd} \right|^2 \right\rangle \right) + \sum_{abcd} \left\langle \sum_{i \neq j} A_i^{ab} A_j^{ab*} \sum_{k \neq l} A_k^{cd} A_l^{cd*} \right\rangle, \tag{3}$$

where the brackets $\langle \cdots \rangle$ mean averaging over all positions of scattering centers. Due to the rapid phase dependence, all the rest terms in $(\delta G)^2$ disappear upon averaging.

The conductance variance (3) contains two contributions which are different by their nature.

The first term in Eq. (3) presents the contribution of nonwave origin and, following Ref. [24], can be referred to as the "incoherent" one. This term is nonzero only provided that both classical trajectories contributing to Eq. (3) pass through the same scattering center [see Fig. 1(a)]. Uncorrelated trajectories govern the square of the disorder-averaged conductance and do not contribute to the variance. The term $\langle (\delta G)^2 \rangle^{\text{incoh}}$ is phase independent and results from fluctuations of the modulus $|A_i^{ab}|$ of the transition amplitude. Physically, the incoherent contribution is due to random variations of classical trajectories in sample-to-sample changes of local scattering properties of the system. This contribution appears only upon averaging over positions of scattering centers. When averaged only over the wave phases (e.g., by changes of the wave frequency or, in electron transport, the energy of carriers), the incoherent contribution does not arise. In this case, the phase-independent terms in Eq. (3) cancel each other.

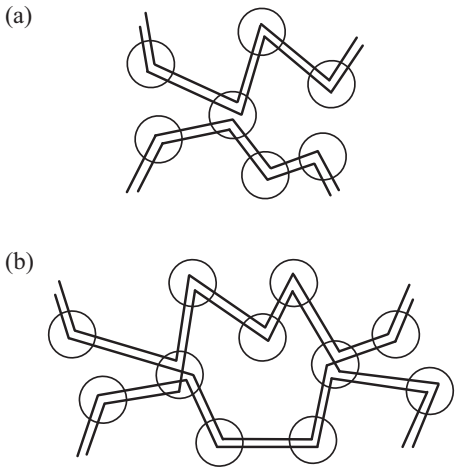

FIG. 1. Examples of wave paths contributing to the conductance variance. Scattering centers are shown by circles. Solid lines denote the transition amplitude or its complex conjugate.

The last term in Eq. (3), the coherent contribution $\langle (\delta G)^2 \rangle^{\text{coh}}$, is the result of interference of the waves propagating along split paths, some parts of which are coincident [an example of such paths is shown in Fig. 1(b)]. This term remains due to those combinations of paths for which the rapid phase dependence cancels out. The effect of UCF [1–5] in the phase-coherent transport is explained just by this configuration of wave paths.

The average conductance $\langle G \rangle$ and the two contributions to the conductance variance $\langle (\delta G)^2 \rangle$ can be easily estimated in the diffusive limit of wave propagation (waveguide length L is much greater than mean free path l). The average conductance $\langle G \rangle$ is proportional to Nl/L where N is the number of propagating modes. This result can be understood by considering the sample as a network of classical parallel- and series-connected parts. Then $\langle G \rangle$ is an additive function of the constituent conductances of N individual modes (or channels). The resistance of one mode (i.e., the reciprocal of its conductance) is the sum of L/l series-connected resistances of the parts into which the sample can be divided.

The incoherent contribution $\langle (\delta G)^2 \rangle^{\text{incoh}}$ can be estimated analogously to $\langle G \rangle$ as a result of summing the fluctuations from uncorrelated parts of length l. In this case, the conductance fluctuations from each mode are added up, while, within a given mode, the conductance fluctuations are expressed in terms of the sum of independent fluctuations of the part's resistances. As a result, the incoherent contribution proves to

be proportional to

$$\langle(\delta G)^2\rangle^{\text{incoh}} \sim N(l/L)^3. \quad (4)$$

Because of the coherence of the waves, the value of $\langle(\delta G)^2\rangle^{\text{coh}}$ is governed by the wave interference in the whole sample, but not by the sum of the contributions from individual parts of the sample. The coherent contribution to the conductance variance can be estimated as the product of the square of the average conductance $\langle G\rangle^2 \sim (Nl/L)^2$ by the probability that the trajectories cross twice each other (see, e.g., [1]), $(L/Nl)^2$. This gives the well-known UCF result

$$\langle(\delta G)^2\rangle^{\text{coh}} \sim 1. \quad (5)$$

The coherent contribution to $\langle(\delta G)^2\rangle$ proves to be a universal quantity of the order of unity which is independent of the number of propagating modes, the size and scattering properties of the system [1–5].

Note that the estimate of the incoherent contribution as the product of the square of the average conductance by the probability of single intersection of two trajectories, gives adequate N dependence but underestimates the exponent of decrease of the conductance variance with increasing the waveguide length L. As follows from the calculations presented below, this is due to the fact that the probability of passing the two rays through the same center differs from the probability of field exchange in splitting the wave paths. In particular, in the case of weak (Born) scattering the probability of passing through the same center vanishes [4]. Therefore, the estimate (4) should be supplemented by a factor which is governed by the strength of single-center scattering. From dimensional reasoning based on the fact that ratio $\langle(\delta G)^2\rangle^{\text{incoh}}/\langle G\rangle^2$ is a wavelength-independent quantity, it is clear that this factor is proportional to $k_0^2\sigma$ where k_0 is the wave number and σ is the single-scattering cross section [36].

As follows from the estimates presented above, there is a range of waveguide lengths where the fluctuations of classical origin are in excess of those from the wave interference. In the case $Nk_0^2\sigma \gg 1$, the incoherent contribution to the conductance variance can be dominant even after the onset of the UCF regime in the phase-coherent transport. In the quasiballistic limit ($L \ll l$), the probability of scattering and, correspondingly, the conductance fluctuations disappear. Thus, from the above reasoning it follows that the conductance variance should peak at subdiffusion scale $L \sim l$, and, under condition $Nk_0^2\sigma \gg 1$, the peak value of $\langle(\delta G)^2\rangle^{\text{incoh}}$ exceeds noticeably the UCF one.

The coherent contribution to $\langle(\delta G)^2\rangle$ results from the so-called speckle [1] arising in the bulk of the sample due to the interference of multiply scattered waves. From sample to sample, this interference pattern changes owing to both variations in the wave phases and local fluctuations of scattering properties of the medium. These latter cause random changes of the modulus $|A_i^{ab}|$ of the transition amplitude and, under conditions of strong single-center scattering, as shown below, are reflected in the value of $\langle(\delta G)^2\rangle^{\text{coh}}$.

Note that the same general reasons as those discussed above underlie sample-to-sample conductance fluctuations in electron transport through a quantum dot (a ballistic cavity with two multichannel contacts) [8]. The classical (i.e., ray- or particlelike) transport is responsible for fluctuations of incoherent origin. In Ref. [8], such fluctuations result from a chaotic walk of classical trajectories undergoing multiple reflections from the cavity walls. The coherent regime of fluctuations is due to the splitting of classical trajectories into interfering components [37]. The splitting can be caused by diffraction from the cavity contacts or by bulk disorder [38]. In the ballistic cavity, depending on the system parameters, either wave interference or classical propagation is realized [8,37]. The separation of these two regimes of wave transport is complete. For a given number of propagating modes N, the incoherent conductance fluctuations are observed in a cavity of relatively small sizes [8]. As the cavity size L increases, the law $\langle(\delta G)^2\rangle^{\text{incoh}} \sim N^4/(k_0L)^2$ is changed by the UCF value $\langle(\delta G)^2\rangle^{\text{coh}} = 1/8$ for a quantum dot. The specific results for a quantum dot [8] and a disordered waveguide (see below) differ because of different patterns of wave propagation in two such systems.

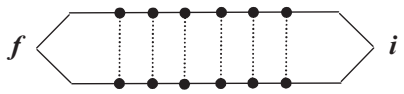

FIG. 2. Diagram for the average conductance. Each circle corresponds to the scattering amplitude (or its complex conjugate). Dashed lines connect identical scatterers. Converging solid lines to a point denotes summation over all outgoing f (or incoming i) modes.

Relatively simple laws of multiple scattering of waves in a disordered waveguide enable us to carry out diagrammatic calculations of the conductance variance analytically with allowance for both mechanisms of fluctuations.

III. DIAGRAMMATIC CALCULATIONS OF THE CONDUCTANCE VARIANCE

Averaging over disorder can be easily performed for great number N of propagating modes ($N = k_0^2A/4\pi$, A is the area of the waveguide cross section). In this case, the summation over modes can be replaced by integration over directions $\mathbf{\Omega}$ of wave propagation (see, e.g., Refs. [14,23]),

$$\sum_a \cdots = \int \frac{Ad\mathbf{q}_a}{(2\pi)^2} \cdots = \frac{k_0^2A}{(2\pi)^2} \int d\mathbf{\Omega}_a |\mu_a| \cdots, \quad (6)$$

where $\mathbf{q}_a$ is the transverse momentum ($q_a < k_0$), $\mu_a = \Omega_{az}$, and the z axis is directed along the waveguide. Hemispheres $\Omega_{az} > 0$ and $\Omega_{az} < 0$ correspond to the waves that propagate in the forward and backward directions, respectively.

Under conditions of weak localization ($G \gg 1$), the value of conductance averaged over an ensemble of disordered samples can be calculated with the standard impurity technique as the sum of ladder diagrams (see Fig. 2). With Eq. (6) the average conductance is written as (see, e.g., [14,23])

$$\langle G\rangle = \frac{N}{\pi} \iint d\mathbf{\Omega}_a d\mathbf{\Omega}_b |\mu_a||\mu_b| I_{ab}(z_f = L|z_i = 0), \quad (7)$$

where propagator $I_{ab}(z|z') = I(z,\mathbf{\Omega}_a|z',\mathbf{\Omega}_b)$ denotes the intensity at depth z in direction $\mathbf{\Omega}_a$ from a source placed at depth z' and emitting waves in direction $\mathbf{\Omega}_b$. The intensity I_{ab} is subject

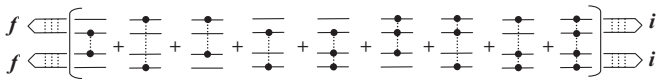

FIG. 3. Diagram for the incoherent contribution to the conductance variance.

to the transport equation [39]

$$\left(\mu_a \frac{\partial}{\partial z} + n\sigma_{\rm tot}\right) I_{ab}(z|z') = \delta(z-z')\delta(\mathbf{\Omega}_a - \mathbf{\Omega}_b) + n\int d\mathbf{\Omega}_c |f_{ac}|^2 I_{cb}(z|z'), \quad (8)$$

where n is the average number of scattering centers per unit volume, $f_{ac} = f(\mathbf{\Omega}_a\mathbf{\Omega}_c)$ is the amplitude of single scattering, $\sigma_{\rm tot} = \sigma + \sigma_{\rm a}$ is the total cross section of interaction, and σ and $\sigma_{\rm a}$ are the cross sections of elastic scattering and absorption, respectively.

A relation similar to Eq. (7) can also be given for the reflectance $\langle R\rangle$. It differs from Eq. (7) only by substitution of $z_f = 0$ for $z_f = L$. For a waveguide with no absorption, the conductance and reflectance are subject to the equality $G + R = N$.

The variance of conductance fluctuations can be expressed in terms of the ensemble-average fourth moment of a wave field [see Eq. (3)] and represented as expansion in orders of interaction between ladder graphs.

A. The incoherent contribution

The most simple diagram that contributes to the conductance variance has the form shown in Fig. 3. The central block entering into this diagram involves all possible connections between four solid lines that denote the wave fields.

Within the Born approximation, only the pair correlations between wave fields are taken into account (see, e.g., Refs. [3,4,14]) and, therefore, the corresponding contribution to $\langle(\delta G)^2\rangle$ is reduced to the first four diagrams. These diagrams, as were shown in Ref. [4], cancel one another provided that the scattering amplitude is taken in the Born approximation. Thus, in such an approximation, this contribution to the conductance variance does not arise.

The situation changes beyond the Born approximation where all graphs shown in Fig. 3 should be taken into account. In this case, the terms entering into the central block can be combined together, to give

$$h_{ab,cd}h^*_{a'b',c'd'}, \quad (9)$$

where

$$h_{aa',bb'} = \frac{2\pi i}{k_0}(f_{ab}\delta_{a'b'} - f^*_{a'b'}\delta_{ab}) + f_{ab}f^*_{a'b'} \quad (10)$$

and asterisks denote the complex conjugation. In Eq. (10), the brief notation $\delta_{ab} = \delta(\mathbf{\Omega}_a - \mathbf{\Omega}_b)$ is used for the delta function. Then, attaching four ladders to the central block, we obtain

$$\langle(\delta G)^2\rangle = A\left(\frac{k_0}{2\pi}\right)^4 n\int_0^L dz \left|\iint d\mathbf{\Omega}_a d\mathbf{\Omega}_b\ I^f_a(z)h_{aa,bb}I^i_b(z)\right|^2. \quad (11)$$

The incoming and outgoing propagators entering into Eq. (11) are expressed in terms of the solution $I_{ab}(z|z')$ to the transport equation (8) as follows:

$$I^i_a(z) = \int d\mathbf{\Omega}_b\, |\mu_b|\, I_{ab}(z|z_i = 0), \quad (12)$$

$$I^f_a(z) = \int d\mathbf{\Omega}_b\, |\mu_b|\, I_{ba}(z_f = L|z). \quad (13)$$

With allowance for the optical theorem

$$\mathrm{Im}\, f_{aa} = \frac{k_0\sigma_{\rm tot}}{4\pi}, \quad (14)$$

the h function appearing in Eq. (11) is written as

$$h_{aa,bb} = -\sigma_{\rm tot}\delta_{ab} + |f_{ab}|^2. \quad (15)$$

The obtained result (11) is the incoherent contribution to the conductance variance $\langle(\delta G)^2\rangle^{\rm incoh}$ which has been discussed qualitatively in Sec. II. If the incident waves differ in frequency, $\langle(\delta G)^2\rangle^{\rm incoh}$ proves to be insensitive to the frequency shift.

The incoherent contribution to $\langle(\delta G)^2\rangle$ describes conductance fluctuations resulting from random variations in the spatial distribution of scatterers. The physical origin of the incoherent contribution to $\langle(\delta G)^2\rangle$ was first pointed out in Ref. [24]. This result is of classical nature and has the same origin as fluctuations of the distribution function obeying the Boltzmann kinetic equation [40]. Equation (11) can also be derived directly from the transport equation (8) as a response of the transmitted flux to variations in the scatterer concentration. Introducing a local perturbation δn in the spatial scatterer distribution $n + \delta n$ we can find the corresponding variation in the intensity propagator $I + \delta I$. Then, under the assumption that the scattering centers are positioned randomly and fluctuations of the scatterer distribution are δ-correlated, we can determine the correlation function $\langle\delta I\delta I\rangle$ and, correspondingly, $\langle(\delta G)^2\rangle^{\rm incoh}$ (see Appendix A).

The h function (10) was first introduced in Ref. [41] where the effects arising beyond the Born approximation in the coherent and incoherent intensity correlations were considered in the plane wave geometry (in this case only a single input mode is excited). Equation (11) extends the corresponding result of Ref. [41] to the case of conductance fluctuations in a disordered waveguide where all input modes are excited.

Note that, within the Born approximation, the above-mentioned cancellation of the first four diagrams (see Fig. 3) occurs only in the Fraunhofer limit $l \gg k_0a^2$ [$l = (n\sigma)^{-1}$ is the elastic mean free path and a is the radius of scattering inhomogeneities] [42]. In the opposite case, $k_0a^2 \gg l$, these diagrams do not cancel [42] and are responsible for long-range intensity correlations in a random medium with extremely large inhomogeneities (e.g., in turbulent atmosphere) [43,44].

The diagrams of the next order in the ladder propagators govern the leading terms of the coherent contribution to $\langle(\delta G)^2\rangle$ (see below). Among these diagrams there are ones that contribute also to the incoherent part of $\langle(\delta G)^2\rangle$. However, the allowance for the diagrams of such a type gives only corrections of order $\sigma/l^2 = 1/(nl^3)$ to the leading term (11).

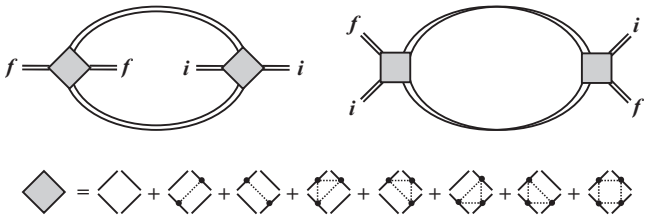

FIG. 4. Diagrams for the coherent contribution to the conductance variance. The paired lines correspond to ladder propagators. The shaded boxes are the Hikami vertices beyond the Born approximation.

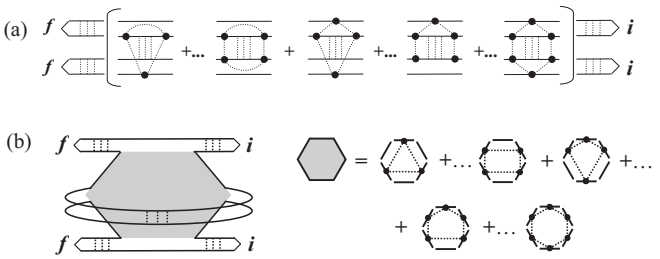

FIG. 5. (a) Additional diagrams contributing to the local term of the conductance variance beyond the Born approximation. (b) Representation of these diagrams in terms of the six-point Hikami box.

B. The coherent contribution

Within the Born approximation, where only pair correlations between wave fields are considered, the conductance variance $\langle(\delta G)^2\rangle$ is governed solely by the coherent contribution (there is no incoherent contribution in such a case). Up to now, all diagrammatic calculations of $\langle(\delta G)^2\rangle^{\rm coh}$ were performed in this approximation (see, e.g., [1–4,14]). The main contribution to $\langle(\delta G)^2\rangle^{\rm coh}$ is governed by two diagrams of the second order in interference events between ladders (see Fig. 4). Each interference event is described by the Hikami vertex [45]. In the presence of time-reversal symmetry, the diagrams shown explicitly in Fig. 4 should be supplemented by their time-reversed counterparts which are obtained by interchanging initial i and final f states in one pair of conjugated wave fields.

Beyond the Born approximation, the well-known diagrams contributing to $\langle(\delta G)^2\rangle^{\rm coh}$ should be generalized with allowance for additional terms [14,41] in the Hikami box (see Fig. 4). It can be shown (see Appendix B) that the contribution from the single Hikami box with four attached ladders is expressed in terms of the product of two h functions [see Eqs. (9) and (10)]. Each term in the Hikami box shown in Fig. 4 corresponds to the product of a certain number of the scattering amplitudes appearing in Eq. (9). This enables us to express the conductance variance in terms of the h functions as a direct extension of the expression [23] for $\langle(\delta G)^2\rangle^{\rm coh}$ obtained within the Born approximation.

Contrary to the treatment carried out within the Born approximation [23], the specific graphs that are responsible for the local term in the expression for $\langle(\delta G)^2\rangle^{\rm coh}$ cannot be included completely into the two-Hikami-box diagrams shown in Fig. 4. A number of additional diagrams [see Fig. 5(a)] which contribute to the local term should be taken into account beyond the Born approximation. These diagrams are among the six-point Hikami box contribution depicted in Fig. 5(b).

The diagrams shown in Figs. 4 and 5 can be evaluated by a straightforward manner. The technique of calculations without resorting to the diffusion approximation has been elaborated in Ref. [23]. In what follows, we take into account the ladders incorporating an arbitrary number of scattering events, among them the graphs without any scattering. These latter describe nonscattered waves. Extending diagrammatic calculations [23] to the case of the Hikami vertices beyond the Born definition (see Appendix B), we derive the following expression for the conductance variance:

$$
\begin{aligned}
\langle(\delta G)^2\rangle^{\rm coh} = {} & \left(\frac{k_0}{2\pi}\right)^4 n^2 \iint_0^L dz\, dz' \int d\mathbf{\Omega}_a \cdots \int d\mathbf{\Omega}_{d_1}\, h_{ab,a_1a_1} h^*_{ab,b_1b_1} h^*_{cd,c_1c_1} h_{cd,d_1d_1} \\
& \times \left\{ I^f_{a_1} I^f_{b_1} I_{ac}\, I_{bd}\, I^i_{c_1} I^i_{d_1} + I^f_{a_1} I^i_{-b_1} I_{ac}\, I_{bd}\, I^f_{-c_1} I^i_{d_1} + \left[I^f_{a_1} I^i_b + I^f_{-b} I^i_{-a_1} \right] I_{ad_1} I_{-b_1-c} \left[I^f_{c_1} I^i_d + I^f_{-d} I^i_{-c_1} \right] \right\} \\
& + \left(\frac{k_0}{2\pi}\right)^2 n \int_0^L dz \iint d\mathbf{\Omega}_a d\mathbf{\Omega}_b \left| \int d\mathbf{\Omega}_{a_1} h_{ab,a_1a_1} \left(I^f_{a_1} I^i_b + I^f_{-b} I^i_{-a_1} \right) \right|^2 I^{(\rm sc)}_{ab}(z|z) \\
& + \left(\frac{k_0}{2\pi}\right)^4 n \int_0^L dz \int d\mathbf{\Omega}_a \cdots \int d\mathbf{\Omega}_{c_1} h_{ab,a_1a_1} \left(I^f_{a_1} I^i_b + I^f_{-b} I^i_{-a_1} \right) h^*_{ac,c_1c_1} \left(I^f_{c_1} I^i_c + I^f_{-c} I^i_{-c_1} \right) h_{bc,b_1b_1} I^{(\rm sc)}_{ab_1}(z|z), \qquad (16)
\end{aligned}
$$

where the function $h_{aa',bb'}$ is defined by Eq. (10), the internal propagator $I_{ab} = I_{ab}(z|z')$ obeys Eq. (8), and the incoming I_i and outgoing I_f propagators are defined by Eqs. (12) and (13), respectively. The propagator $I^{(\rm sc)}_{ab}$ is the intensity of waves that undergo one or more acts of scattering.

The change of sign in a subscript of any propagator entering into Eq. (16) implies the reverse of the direction (i.e., substitution of $-\mathbf{\Omega}_a$ for $\mathbf{\Omega}_a$ into the propagator). The incoming and outgoing propagators appearing in Eq. (16) with subscripts $\pm a_1$, $\pm b$, $\pm b_1$ are functions of z, while those with subscripts $\pm c_1$, d_1, $\pm d$ are functions of z'. The propagators entering into the local term [see the third and fourth lines of Eq. (16)] are functions of z.

Equation (16) has the presented form provided that the time-reversal symmetry is not violated. The terms that contain products of the incoming and outgoing propagators with subscripts of opposite sign (e.g., $I^f_{a_1} I^i_b [\cdots] I^f_{-d} I^i_{-c_1}$) correspond to the cooperon contribution. The cooperon contribution includes

the maximally crossed internal graphs and, in the low-order scattering limit, the internal graphs that describe the waves propagating in opposite directions [23].

Expressions similar to Eqs. (11) and (16) are also valid for the reflection geometry. The reflectance variance $\langle(\delta R)^2\rangle$ differs from Eqs. (11) and (16) only by substitution of $z_f = 0$ for $z_f = L$ in all outgoing propagators.

Equations (11) and (16) are the principal results of our work. Formula (16) for $\langle(\delta G)^2\rangle^{\rm coh}$ generalizes the results derived previously [1,4,14,23] in two aspects. On one hand, Eq. (16) extends the result of Ref. [23] beyond the Born approximation. On the other, Eq. (16) (as well as the corresponding formula of Ref. [23]) generalizes the result of the diffusion approximation [1,4,14], much as the transport equation generalizes the equation of diffusion. Equation (16) establishes the interrelation between the conductance variance and the characteristics of scattering centers of the disordered system, and enables us to study evolution of the fluctuations in going from the quasiballistic propagation to the diffusive regime.

In practice, the incoherent and coherent contributions to $\langle(\delta G)^2\rangle$ can be separated from each other with the frequency dependence of the conductance fluctuations. If the incident waves differ in frequency, the correlation function of conductance fluctuations $\langle\delta G(\omega_0 + \Delta\omega/2)\delta G(\omega_0 - \Delta\omega/2)\rangle$ can be introduced [14]. The incoherent contribution to the correlation function is independent of the frequency shift $\Delta\omega$, while the coherent one falls off with increasing $\Delta\omega$. Equation (16) can easily be extended to determine the correlation function $\langle\delta G(\omega_0 + \Delta\omega/2)\delta G(\omega_0 - \Delta\omega/2)\rangle$. The frequency shift $\Delta\omega$ appears only in the internal propagators entering into Eq. (16). The internal propagators in the second line of Eq. (16) take the form $I_{ac}I_{bd} = I_{ac}(\Delta\omega)I_{bd}(-\Delta\omega)$ and $I_{ad_1}I_{-b_1-c} = {\rm Re}\{I_{ad_1}(\Delta\omega)I_{-b_1-c}(\Delta\omega)\}$. The internal propagator in the local terms transforms to ${\rm Re}\{I_{ab}(\Delta\omega)\}$. The propagator $I_{ab}(\Delta\omega) = I(z,\mathbf{\Omega}_a|z',\mathbf{\Omega}_b,\Delta\omega)$ obeys the transport equation that is obtained from Eq. (8) by substitution of complex absorption coefficient $(n\sigma_a + i\Delta\omega/c)$ for $n\sigma_a$ (c is the velocity of waves).

IV. CROSSOVER BETWEEN THE QUASIBALLISTIC AND DIFFUSIVE REGIMES

As an illustration of application of Eqs. (11) and (16) to calculating the conductance variance beyond the diffusion approximation, we find $\langle(\delta G)^2\rangle$ within the two-stream version of the discrete-ordinate method [39]. This simplest model enables us to perform integration in Eqs. (11) and (16) explicitly and to derive an analytical result for $\langle(\delta G)^2\rangle$ which describes the crossover between the quasiballistic and diffusive regimes.

Within this approach, each integral over $\mathbf{\Omega}$ is supposed to be equal to the sum of the values of an integrand quantity at $\Omega_z = \pm\mu_0$,

$$\int d\mathbf{\Omega}_a I(z,\mathbf{\Omega}_a) = 2\pi I_+(z) + 2\pi I_-(z), \tag{17}$$

where $I_\pm(z) = I(z,\Omega_z = \pm\mu_0)$, and $\pm\mu_0$ are the discrete ordinates [39]. We apply this rule to evaluating each integral over directions appearing in Eqs. (11) and (16).

Most of the calculations of the conductance variance were carried out within the model of pointlike centers (see, e.g., [2–4,14]). In this case, the scattering amplitude is independent of directions $f_{ab} = f$ and

$$h_{aa',bb'} = \frac{2\pi i f}{k_0}(\delta_{a'b'} - \delta_{ab}) + (|f|^2 - \sigma_{\rm tot}\delta_{ab}). \tag{18}$$

The first term in Eq. (18) can be considered responsible for fluctuations of interference nature. This term differs from that obtained within the Born approximation only by substitution of the exact scattering amplitude for the Born one. The second term in Eq. (18) is coincident with Eq. (15) and, therefore, can be thought of as resulting from variations in number of scatterers per unit volume.

Substituting the propagators calculated within two-stream approximation [23] to Eqs. (11) and (16), we arrive at the following result for the conductance variance:

$$\langle(\delta G)^2\rangle = \langle(\delta G)^2\rangle^{\rm incoh} + \langle(\delta G)^2\rangle^{\rm coh}, \tag{19}$$

where the incoherent and the coherent contributions are equal to

$$\langle(\delta G)^2\rangle^{\rm incoh} = N\frac{k_0^2\sigma}{4\pi}\frac{2s}{(1+s)^4}, \tag{20}$$

$$\begin{aligned}\langle(\delta G)^2\rangle^{\rm coh} = {}& \frac{2}{15}\left(1 - \frac{1+6s}{(1+s)^6}\right) \\ & - \frac{k_0^2\sigma}{4\pi}\frac{4s}{(1+s)^4}\left(1 - \frac{1}{(1+s)^2}\right) \\ & + \left(\frac{k_0^2\sigma}{4\pi}\right)^2\frac{4s}{(1+s)^4}\left(1 - \frac{2-s}{2(1+s)^2}\right),\end{aligned} \tag{21}$$

$s = (1/2\mu_0)(L/l)$ and N is the number of propagating modes.

The first term in Eq. (21) coincides with the result obtained previously with the RMT approach [34,35]. As was shown in Ref. [23], this term is also derived by the impurity diagrammatic technique within the Born approximation for the Hikami box [46].

The incoherent contribution (20) and the second and third terms appearing in Eq. (21) arise beyond the Born approximation. All these terms are proportional to powers of $k_0^2\sigma/4\pi$. As has already been discussed above (see Sec. II A and Appendix A), the incoherent contribution is due to the scattering coefficient fluctuations caused by random variations in the scatterer spatial distribution. The same origin underlies the last term in the coherent contribution (21). This term can be construed as resulting from perturbation of the interference pattern [47] by random variations in the scatterer distribution. The second term in Eq. (21) is due to the combined effect of the wave interference and the above-mentioned perturbation of the interference pattern on conductance fluctuations. The negative sign of this term comes from the fact that a local deviation in the scatterer concentration leads to changes of opposite signs in the coherent (nonscattered) wave field and the scattered one.

From Eqs. (19)–(21) it follows that the variance $\langle(\delta G)^2\rangle$ peaks at subdiffusion scales $s \sim 1$. In the limit of a long waveguide $s \gg 1$, the variance of the conductance fluctuations

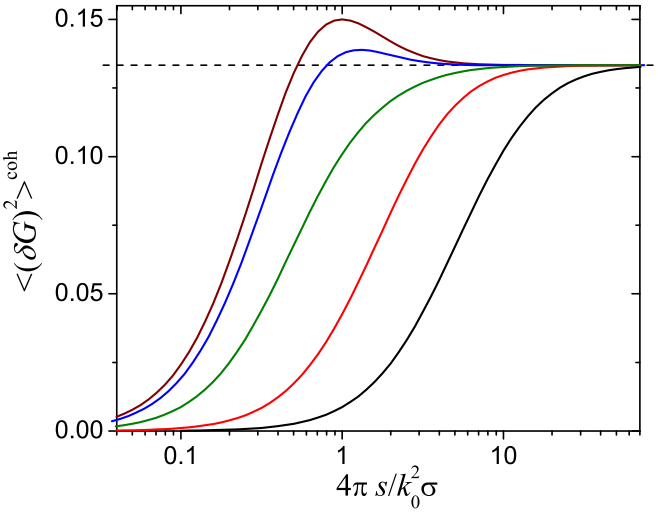

FIG. 6. Coherent contribution to the conductance variance as a function of the waveguide length. From lower to upper curves $k_0^2\sigma/(4\pi) = 0.1$, 0.5, 0.8, 0.95, and 1.0. The horizontal line is the UCF value 2/15.

approximates

$$\langle(\delta G)^2\rangle = \frac{2}{15} + N\frac{k_0^2\sigma}{2\pi}\frac{1}{s^3} + \cdots \tag{22}$$

and always tends to the UCF value from above.

The dependence of the conductance variance on the waveguide length is illustrated in Figs. 6 and 7.

The first of the figures shows the impact of the scattering strength on the coherent contribution to $\langle(\delta G)^2\rangle$. For pointlike scatterers the scattering amplitude can be written in the form

$$f = -\frac{\alpha}{1 + ik_0\alpha}, \tag{23}$$

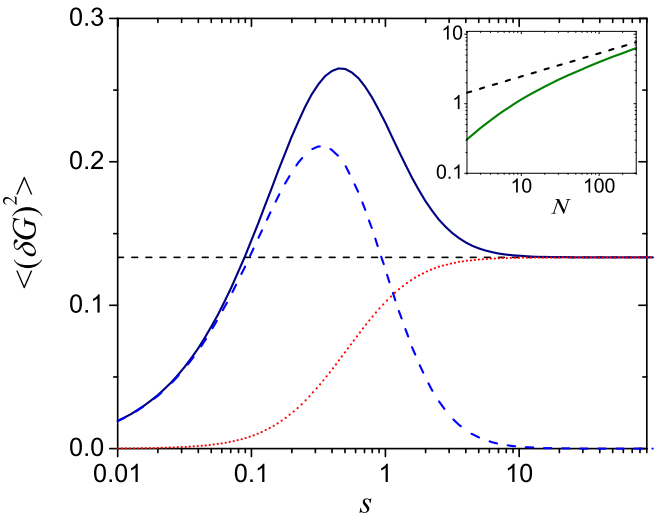

FIG. 7. Length dependence of the conductance variance (solid curve). The coherent and incoherent contributions are shown by dotted and dashed curves, respectively. $N = 10$, $k_0^2\sigma/(4\pi) = 0.1$. The inset shows the waveguide length s_* at which the coherent contribution becomes equal to the incoherent one versus N. The dashed line is the law $s_* = [15Nk_0^2\sigma/(4\pi)]^{1/3}$.

where α is the scattering length [48]. The scattering strength is characterized by parameters $k_0\alpha$ or $k_0^2\sigma/(4\pi) = k_0^2\alpha^2/(1 + k_0^2\alpha^2)$. In the Born limit, the both parameters are much less than unity, while in the resonance limit $k_0\alpha \gg 1$ and $k_0^2\sigma/(4\pi) = 1$.

For different values of the parameter $k_0^2\sigma/(4\pi)$, the length dependence of the conductance variance is illustrated in Fig. 6. The variable $s/(k_0^2\sigma/4\pi)$ plotted on the abscissa axis is independent of the scattering cross-section σ. Therefore, the presented graphs give insight into changes of the variance $\langle(\delta G)^2\rangle^{\rm coh}$ with increasing the scattering strength. As follows from Fig. 6, the effect of strong scattering manifests itself at relatively short waveguide lengths. The influence of the non-Born terms of Eq. (21) increases with the scattering strength, resulting in an appearance of the local maximum in the length dependence of $\langle(\delta G)^2\rangle^{\rm coh}$. For the limiting value $\sigma = 4\pi/k_0^2$, the conductance variance peaks at $s = 1$ and its maximum value is $\langle(\delta G)^2\rangle^{\rm coh} = 3/20$.

The total value of the conductance variance (19) as a function of the waveguide length is shown in Fig. 7. For $Nk_0^2\sigma/4\pi > 1$, the variance peaks at $s \approx 1/3$, and its maximum value is approximately $Nk_0^2\sigma/2\pi$ times greater than the UCF one. The incoherent contribution proves to be dominant at scales $s \leqslant (Nk_0^2\sigma)^{1/3}$. The coherent contribution to the conductance fluctuations becomes principal in the limit $s > (Nk_0^2\sigma)^{1/3}$ where $\langle(\delta G)^2\rangle$ is described by the UCF.

From Eqs. (20) and (21) it follows that the ratio $\langle(\delta G)^2\rangle^{\rm coh}/\langle(\delta G)^2\rangle^{\rm incoh}$ is of order $s/(Nk_0^2\sigma/4\pi)$ at $s \ll 1$. This result is in agreement with the estimates obtained in Ref. [24]. However, the opposite conclusion was drawn in Ref. [24] regarding the role of the incoherent contribution to $\langle(\delta G)^2\rangle$. The matter is that, in Ref. [24], the number of modes were moderate and the scattering potential was assumed to be weak (i.e., the parameter $Nk_0^2\sigma/4\pi$ was thought of to be small).

V. DIFFUSIVE REGIME

For a long waveguide $L \gg l$, the main contributions to the integrals over z and z' in Eqs. (11) and (16) are governed by the distances that are far away from the input and output waveguide boundaries, and the diffusion approximation can be applied to calculating the intensity propagators appearing in these equations. In this case, the propagators turn out to depend only slightly on the directions and can be expanded in terms of the Legendre polynomials [39].

Substituting the diffusion expansion of the incoming and outgoing propagators (see, e.g., Ref. [23]) into Eq. (11) and using the relation

$$\int d\mathbf{\Omega}_c\, h_{ab,cc} I_c^{i,f}(z) = \frac{2\pi i}{k_0}(f\mu_b - f^*\mu_a)\frac{3J_{i,f}(z)}{4\pi}, \tag{24}$$

where

$$J_{i,f}(z) = \int d\mathbf{\Omega}_a \mu_a I_a^{i,f}(z), \tag{25}$$

we arrive at the following result for the incoherent contribution:

$$\langle(\delta G)^2\rangle^{\rm incoh} = \frac{9}{(2\pi)^4}\frac{k_0^2\sigma}{4\pi}N\int_0^L \frac{dz}{l} J_f^2(z) J_i^2(z). \tag{26}$$

Calculations with Eq. (26) give

$$\langle(\delta G)^2\rangle^{\rm incoh} = \frac{16}{9}\frac{k_0^2\sigma}{4\pi}N\left(\frac{l}{L}\right)^3. \tag{27}$$

This result is in agreement with the leading term of expansion of Eq. (20) in inverse powers of the waveguide length L.

Application of the diffusion approximation to Eq. (16) gives rise, as a first approximation, to the well-known diffusion formula for the conductance variance (see, e.g., Refs. [14,23,49])

$$\begin{aligned}\langle(\delta G)^2\rangle^{\rm coh} = \left(\frac{3}{32\pi^3 l}\right)^2 \iint_0^L dz dz' \big\{ & J_f^2(z)\Phi^2(z|z')J_i^2(z') + J_f(z)J_i(z)\Phi^2(z|z')J_f(z')J_i(z') \\ & + [J_f(z)\Phi_i(z) - J_i(z)\Phi_f(z)]J(z|z')J(z'|z)[J_f(z')\Phi_i(z') - J_i(z')\Phi_f(z')]\big\} \\ & + \frac{6}{(4\pi)^5 l}\int_0^L dz[J_f(z)\Phi_i(z) - J_i(z)\Phi_f(z)]^2\Phi(z|z),\end{aligned} \tag{28}$$

where

$$\Phi_{i,f}(z) = \int d\mathbf{\Omega}_a I_a^{i,f}(z), \tag{29}$$

$$\Phi(z|z') = \iint d\mathbf{\Omega}_a d\mathbf{\Omega}_b I_{ab}(z|z'), \tag{30}$$

$$J(z|z') = \iint d\mathbf{\Omega}_a d\mathbf{\Omega}_b\, \mu_a I_{ab}(z|z'). \tag{31}$$

Within the diffusion approximation, the current J is expressed in terms of the derivative of the density Φ,

$$J_{i,f}(z) = \mp\frac{l}{3}\frac{\partial\Phi_{i,f}(z)}{\partial z}, \quad J(z|z') = -\frac{l}{3}\frac{\partial\Phi(z|z')}{\partial z}.$$

Calculations with Eq. (28) give the UCF result $\langle(\delta G)^2\rangle^{\rm coh} = 2/15$.

Corrections to Eq. (28), however, cannot be found within the standard diffusion approximation. The matter is that these corrections are governed by the contributions to the integrals over z and z' in Eq. (16) from rather short wave paths, i.e., $|z - z'| \leqslant l$. Allowance for such wave paths is beyond the diffusion approximation. In addition to the two terms taken into account in the diffusion approximation, the terms of higher order should be kept in the propagator expansion in the Legendre polynomials.

So, although the diffusion approach enables one to take into account the effect of the scatterer concentration fluctuations on the single-Hikami-box contribution [41], this approach fails in calculating the corresponding corrections to the diffusion formula for $\langle(\delta G)^2\rangle^{\rm coh}$.

The results obtained above, Eqs. (26)–(28), can easily be extended to an arbitrary single-scattering law. In this case, the right-hand side of Eq. (24) is replaced by

$$\left(\frac{2\pi i}{k_0}(f_{ab}\mu_b - f_{ab}^*\mu_a) + \int d\mathbf{\Omega}_{a_1}\mu_{a_1} f_{aa_1} f_{a_1 b}^*\right)\frac{3J_{i,f}(z)}{4\pi}. \tag{32}$$

With allowance for Eq. (32) and the generalized optical theorem [48]

$$\int d\mathbf{\Omega}_{a_1} f_{aa_1} f_{a_1 b}^* = \frac{2\pi i}{k_0}(f_{ab}^* - f_{ab}), \tag{33}$$

Eqs. (26)–(28) are transformed as follows: the transport cross section

$$\sigma_{\rm tr} = \int d\mathbf{\Omega}_a(1 - \mathbf{\Omega}_a\mathbf{\Omega}_b)|f_{ab}|^2 \tag{34}$$

and transport mean free path $l_{\rm tr} = (n\sigma_{\rm tr})^{-1}$ should be substituted to Eqs. (26)–(28) for σ and l, respectively.

The above-considered effects caused by strong single-center scattering can be directly observed in microwave experiments similar to those outlined in Refs. [10,11]. The coherent and incoherent contributions can be separated from each other by the dependence of conductance fluctuations on the frequency shift $\Delta\omega$ between the incident waves (see Sec. II B). For $\Delta\omega = 0$, the conductance variance is equal to the sum of both contributions. As $\Delta\omega$ increases, only the incoherent one survives. The appreciable magnitude of the frequency-independent component of fluctuations measured in Ref. [11] can be explained just by this contribution. With allowance for absorption present in experiment [11], Eqs. (26) and (28) yield

$$\frac{\langle(\delta G)^2\rangle^{\rm incoh}}{\langle(\delta G)^2\rangle^{\rm coh}} = \frac{32}{9}\frac{k_0^2\sigma_{\rm tr}}{4\pi}N\frac{l_{\rm tr}^3}{Ll_D^2}, \tag{35}$$

where $l_D = (l_a l_{\rm tr}/3)^{1/2}$, and l_a is the absorption mean free path. In Eq. (35), the waveguide length L is assumed to be much greater than l_D. For the parameter values taken from the data of Ref. [11], Eq. (35) gives the ratio equal to 0.2. The ratio of the $\Delta\omega$-independent part to the $\Delta\omega$-dependent one measured in Ref. [11] approximates 0.3 that correlates well with our theoretical estimate.

VI. CONCLUSIONS

In conclusion, we have studied the effect of strong single scattering on the mesoscopic conductance fluctuations in a quasi-1D disordered system. The conductance fluctuations have been shown to be enhanced in the crossover between ballistic and diffusive regimes and can noticeably exceed the UCF value. The Hikami vertex appearing in the diagrammatic calculations of the conductance variance has been extended beyond the standard Born definition. Our result relates the variance of conductance fluctuations to the characteristics of a disordered system (single center scattering amplitude, the number of propagating modes, etc.) and enables us to

find the conditions under which the conductance variance exceeds the UCF value.

Going beyond the Born approximation for the Hikami vertex has enabled us to take into account the effect of random variations in the scatterer concentration on sample-to-sample conductance fluctuations. Due to this effect, the incoherent contribution to the variance arises. This contribution is proportional to the number of propagating modes and can be dominant in the crossover regime resulting in appearance of the pronounced maximum in the length dependence of the conductance variance. In the diffusive limit, the incoherent contribution decreases as $1/L^3$. Beyond the Born approximation, additional terms appear in the coherent contribution to the conductance variance along with the well-known term obtained within both the RMT approach [34,35] and the diagrammatic calculations for pointlike scatterers [23]. In the limit of resonant scatterers, the maximum value of the coherent contribution to the conductance variance is greater than the UCF value and achieved at subdiffusion scales $L \sim l$.

The results presented above can be useful for understanding how the specific features of disorder reveal themselves in transport through mesoscopic systems.

ACKNOWLEDGMENT

We acknowledge support from the MEPhI Academic Excellence Project (Contract 02.a03.21.0005, 27.08.2013).

APPENDIX A: DERIVATION OF THE INCOHERENT CONTRIBUTION FROM THE TRANSPORT EQUATION

Response of the conductance to variations in the impurity concentration can be derived directly from the transport equation.

Let us introduce a local perturbation δn in the spatial impurity distribution. Then, substituting $n+\delta n$ for n into Eq. (8) we obtain the transport equation for the perturbed intensity propagator $I+\delta I$ where I is a solution of the nonperturbed equation. Neglecting the nonlinear terms containing the product $\delta I \delta n$, we obtain the transport equation for δI within a linear approximation with respect to δn,

$$\left(\Omega_{az}\frac{\partial}{\partial z}+n\sigma_{\rm tot}\right)\delta I_{ab}(z|z') = n\int d\mathbf{\Omega}_c \frac{d\sigma}{d\Omega}(\mathbf{\Omega}_a\mathbf{\Omega}_c)\delta I_{cb}(z|z') + \delta n\left(-\sigma_{\rm tot}+\int d\mathbf{\Omega}_c\frac{d\sigma}{d\Omega}(\mathbf{\Omega}_a\mathbf{\Omega}_c)I_{cb}(z|z')\right). \quad \text{(A1)}$$

Considering the last term that contains a perturbation δn as a source we can find δI in the following form:

$$\delta I_{ab} = \int_0^L dz\delta n \iint d\mathbf{\Omega}'_a d\mathbf{\Omega}'_b\ I_{aa'}(|f_{a'b'}|^2-\sigma_{\rm tot}\delta_{a'b'})I_{b'b}. \quad \text{(A2)}$$

Using Eq. (A2) we can relate the correlation function $\langle\delta I\delta I\rangle$ and, correspondingly, $\langle(\delta G)^2\rangle$ to the correlation function $\langle\delta n(z)\delta n(z')\rangle$. Under the assumption that fluctuations of the scatterer distribution are δ-correlated, we arrive at Eq. (11).

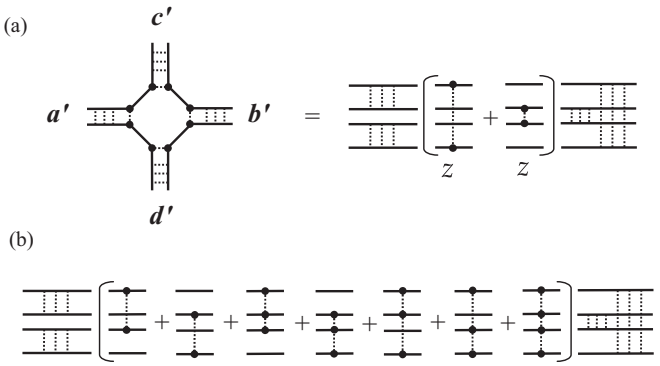

FIG. 8. Hikami box with four attached ladder propagators. (a) Empty box contribution. (b) Extra-scattering contribution beyond the Born approximation.

APPENDIX B: EXTENDING THE DIAGRAMMATIC CALCULATIONS BEYOND THE BORN APPROXIMATION

The variance of conductance fluctuations can be expressed in terms of the ensemble-average fourth moment of a wave field and represented as expansion in orders of interference between ladder graphs. Each interference event between the ladders contains the Hikami vertex [45].

First we consider the diagram that involves the single Hikami vertex with four attached ladder propagators. This diagram can be thought as a building block appearing in the diagrams shown in Fig. 4. According to Ref. [23] the contribution from the "empty" Hikami box can be presented in the form

$$\left(\frac{\pi}{N}\right)^3 n\int dz\iint d\mathbf{\Omega}_a d\mathbf{\Omega}_b |f_{ab}|^2\, I_{a'a}(\cdot\cdot|z)I_{b'a}(\cdot\cdot|z) \times [I_{bc'}(z|\cdot\cdot)I_{ad'}(z|\cdot\cdot)+I_{ac'}(z|\cdot\cdot)I_{bd'}(z|\cdot\cdot)], \quad \text{(B1)}$$

where $N=k_0^2A/4\pi$ is the number of propagating modes. As has been shown in Ref. [23], the waves contributing to the empty box propagate in an identical mode (or in a given direction [50]). Therefore, we can establish the sequence of scattering events along the z axis. Separating one scattering event from either of two ladder propagators attached to the opposite ends of the Hikami box we can display the contribution (B1) in the diagrammatic form shown in Fig. 8(a). The mutual arrangement of the scattering events depicted in the second two graphs of Fig. 8(a) results from compensating the phases of Green functions [23,50].

The single-Hikami diagrammatic block that involves the Hikami box with extra scattering can be presented in the same manner as in Fig. 8(a). Beyond the Born approximation, in addition to pair correlations, the correlations between three and four fields should be also taken into account [see Fig. 8(b)].

The sum of the graphs shown in Fig. 8 differs from the incoherent diagrammatic contribution (see Fig. 8) only by the manner of attaching the ladder propagators to the central block. As a result the single-Hikami-box contribution can be

expressed in terms of the above-introduced quantity hh^*:

$$\left(\frac{k_0}{2\pi}\right)^2\left(\frac{\pi}{N}\right)^3 n\int dz\iiiint d\boldsymbol{\Omega}_a d\boldsymbol{\Omega}_b d\boldsymbol{\Omega}_{a_1} d\boldsymbol{\Omega}_{b_1} I_{a'a_1}(\cdot\cdot|z) \times I_{b'b_1}(\cdot\cdot|z) h_{a_1a_1,ab} h^*_{b_1b_1,ab} I_{ac'}(z|\cdot\cdot) I_{bd'}(z|\cdot\cdot). \tag{B2}$$

The obtained result is confirmed by straightforward calculations of each diagram shown in Fig. 8. The propagators entering into Eq. (B2) can also be "read" in the reverse order [i.e., propagators $I_{a'a_1}(\cdot\cdot|z)$ and $I_{bd'}(z|\cdot\cdot)$ are replaced by $I_{a_1a'}(z|\cdot\cdot)$ and $I_{d'b}(\cdot\cdot|z)$, respectively]. In addition, Eq. (B2) can be rewritten in the form that is obtained by interchanging pairs a', b' and c', d'. All these representations are equivalent to each other and applied to evaluating the diagrams of the second order in the Hikami vertex.

So, to generalize the contribution from the two-Hikami-box diagrams to $\langle(\delta G)^2\rangle$ beyond the Born approximation, we should substitute

$$\left(\frac{k_0}{2\pi}\right)^2\iint d\boldsymbol{\Omega}_{a_1} d\boldsymbol{\Omega}_{b_1}\, I_{a'a_1}(\cdot\cdot|z)\, I_{b'b_1}(\cdot\cdot|z) h_{a_1a_1,ab} h^*_{b_1b_1,ab} \tag{B3}$$

for

$$|f_{ab}|^2[I_{a'a}(\cdot\cdot|z) - I_{a'b}(\cdot\cdot|z)]\,[I_{b'a}(\cdot\cdot|z) - I_{b'b}(\cdot\cdot|z)] \tag{B4}$$

into Eq. (5) of Ref. [23]. The rule given by Eqs. (B3) and (B4) is valid with one proviso regarding the local term entering into the expression for $\langle(\delta G)\rangle^2$.

Within the Born approximation the variance $\langle(\delta G)\rangle^2$ can be described completely by the diagrams shown in Fig. 4. As was shown in Ref. [23] we need not introduce particular diagrams containing only one internal ladder propagator and the six-point Hikami vertex. Such diagrams are already contained among the diagrams depicted in Fig. 4. They correspond to the pair of nonscattered waves in either of two internal ladders.

Beyond the Born approximation the situation changes. Depending on the arrangement of scattering events in the Hikami boxes, the diagrams shown in Fig. 4 make a contribution either to the nonlocal term or to the local ones appearing in Eq. (16). However, the two-Hikami-box diagrams describe only a part of the local term containing three h functions. Beyond the Born approximation, there are a number of diagrams which are not managed to present as the diagrams with two four-point Hikami boxes. The diagrams of such a type are depicted in Fig. 5. We can also present these additional diagrams in terms of the six-point Hikami box with one internal ladder propagator [see Fig. 5(b)]. These diagrams make a contribution only to the local term with three h functions.

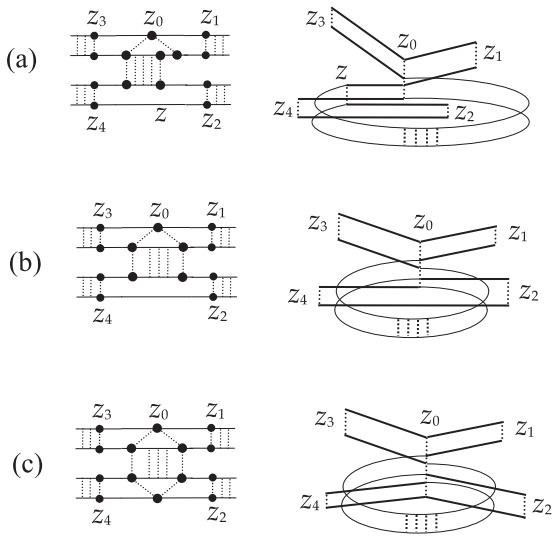

FIG. 9. Examples of the diagrams contributing to the local term with three h functions. The right graphs show the spatial arrangement of scattering events in the diagrams.

The diagrams contributing to the local term with three h functions are exemplified in Fig. 9. The spatial arrangement of the scattering events appearing in these diagrams is sought from the condition of compensating the Green function phases (this procedure is a consequence of evaluating the corresponding integrals with the stationary phase method [39] and has already been discussed in Ref. [23]). The first graph shown in Fig. 9(a) originates from the two-Hikami-box diagram with the pair of nonscattered waves in either of two internal propagators. The specific arrangement of scattering events shown in Fig. 9(a) contributes to the local term. The examples of the arrangement of scattering events in the additional diagrams contained in the six-point Hikami box are illustrated in Figs. 9(b) and 9(c).

[1] E. Akkermans and G. Montambaux, *Mesoscopic Physics of Electrons and Photons* (Cambridge University Press, Cambridge, 2011).
[2] B. L. Altshuler, JETP Lett. **41**, 648 (1985); P. A. Lee and A. D. Stone, Phys. Rev. Lett. **55**, 1622 (1985).
[3] P. A. Lee, A. D. Stone, and H. Fukuyama, Phys. Rev. B **35**, 1039 (1987).
[4] C. L. Kane, R. A. Serota, and P. A. Lee, Phys. Rev. B **37**, 6701 (1988).
[5] S. Washburn and R. A. Webb, Rep. Prog. Phys. **55**, 1311 (1992).
[6] P. Mohanty and R. A. Webb, Phys. Rev. Lett. **88**, 146601 (2002).
[7] T. Ludwig, Ya. M. Blanter, and A. D. Mirlin, Phys. Rev. B **70**, 235315 (2004).
[8] J. Tworzydlo, A. Tajic, and C. W. J. Beenakker, Phys. Rev. B **69**, 165318 (2004); Ph. Jacquod and E. V. Sukhorukov, Phys. Rev. Lett. **92**, 116801 (2004).
[9] F. Scheffold and G. Maret, Phys. Rev. Lett. **81**, 5800 (1998).
[10] P. Sebbah, B. Hu, A. Z. Genack, R. Pnini, and B. Shapiro, Phys. Rev. Lett. **88**, 123901 (2002).
[11] A. A. Chabanov, N. P. Tregoures, B. A. van Tiggelen, and A. Z. Genack, Phys. Rev. Lett. **92**, 173901 (2004).
[12] N. Cherroret, A. Pena, A. A. Chabanov, and S. E. Skipetrov, Phys. Rev. B **80**, 045118 (2009).
[13] P. A. Mello, E. Akkermans, and B. Shapiro, Phys. Rev. Lett. **61**, 459 (1988).
[14] M. C. W. van Rossum and Th. M. Nieuwenhuizen, Rev. Mod. Phys. **71**, 313 (1999).

[15] H. Tamura and T. Ando, Phys. Rev. B **44**, 1792 (1991).
[16] K. Nikolic and A. MacKinnon, Phys. Rev. B **50**, 11008 (1994).
[17] T. N. Todorov, Phys. Rev. B **54**, 5801 (1996).
[18] Y. Takagaki and K. H. Ploog, Phys. Rev. B **63**, 125311 (2001).
[19] T. Ando, J. Phys. Soc. Jpn. **73**, 1895 (2004).
[20] T. Markussen, R. Rurali, A.-P. Jauho, and M. Brandbyge, Phys. Rev. Lett. **99**, 076803 (2007).
[21] J. Feilhauer and M. Mosko, Phys. Rev. B **83**, 245328 (2011).
[22] F. Iori, S. Ossicini, and R. Rurali, J. Appl. Phys. **116**, 074303 (2014).
[23] V. V. Marinyuk and D. B. Rogozkin, Phys. Rev. B **91**, 125125 (2015).
[24] L. I. Glazman and M. Jonson, Phys. Rev. B **44**, 3810 (1991).
[25] A. M. See, I. Pilgrim, B. C. Scannell, R. D. Montgomery, O. Klochan, A. M. Burke, M. Aagesen, P. E. Lindelof, I. Farrer, D. A. Ritchie, R. P. Taylor, A. R. Hamilton, and A. P. Micolich, Phys. Rev. Lett. **108**, 196807 (2012).
[26] A. P. Micolich, A. M. See, B. C. Scannell, C. A. Marlow, T. P. Martin, I. Pilgrim, A. R. Hamilton, H. Linke, and R. P. Taylor, Fortschr. Phys. **61**, 332 (2013).
[27] A. M. See, A. R. Hamilton, A. P. Micolich, M. Aagesen, and P. E. Lindelof, Phys. Rev. B **91**, 085417 (2015)
[28] Regarding the impact of strong scatterers on the average conductivity of mesoscopic systems, see, e.g., A. D. Mirlin, D. G. Polyakov, F. Evers, and P. Wolfle, Phys. Rev. Lett. **87**, 126805 (2001); P. M. Ostrovsky, M. Titov, S. Bera, I. V. Gornyi, and A. D. Mirlin, *ibid.* **105**, 266803 (2010).
[29] J. Pelz and J. Clarke, Phys. Rev. B **36**, 4479(R) (1987).
[30] S. Hershfield, Phys. Rev. B **37**, 8557 (1988).
[31] N. Giordano and E. R. Schuler, Phys. Rev. B **41**, 11822 (1990).
[32] Yu. M. Galperin and V. I. Kozub, Europhys. Lett. **15**, 631 (1991); V. I. Kozub and A. A. Krokhin, J. Phys.: Condens. Matter **5**, 9135 (1993).
[33] H. Hennig, R. Fleischmann, L. Hufnagel, and T. Geisel, Phys. Rev. E **76**, 015202(R) (2007).
[34] P. A. Mello, Phys. Rev. Lett. **60**, 1089 (1988); P. A. Mello and A. D. Stone, Phys. Rev. B **44**, 3559 (1991).
[35] A. Garcia-Martin, F. Scheffold, M. Nieto-Vesperinas, and J. J. Saenz, Phys. Rev. Lett. **88**, 143901 (2002).
[36] According to this estimate, the probability that two rays pass through the same center is the reciprocal of the total number of centers in the sample.
[37] O. Agam, I. Aleiner, and A. Larkin, Phys. Rev. Lett. **85**, 3153 (2000).
[38] For a review, see E. V. Sukhorukov and O. M. Bulashenko, Phys. Rev. Lett. **94**, 116803 (2005); F. Aigner, S. Rotter, and J. Burgdorfer, *ibid.* **94**, 216801 (2005); where crossover from classical to quantum transport was considered in the context of shot noise in chaotic cavities.
[39] A. Ishimaru, *Wave Propagation and Scattering in Random Media*, IEEE Press Series on Electromagnetic Wave Theory (Wiley, New York, 1999).
[40] E. M. Lifshitz and L. P. Pitaevskii, *Physical Kinetics: Volume 10 of Course of Theoretical Physics* (Pergamon Press, New York, 1981).
[41] D. B. Rogozkin and M. Yu. Cherkasov, Phys. Lett. A **214**, 292 (1996); D. B. Rogozkin, JETP **84**, 916 (1997).
[42] D. B. Rogozkin and M. Yu. Cherkasov, Phys. Lett. A **178**, 431 (1993).
[43] A. M. Prokhorov, F. V. Bunkin, K. S. Gochelashvily, and V. I. Shishov, Proc. IEEE **63**, 790 (1975).
[44] J. L. Codona, D. B. Creamer, S. M. Flatte, R. G. Frehlich, and F. S. Henyey, Radio Sci. **21**, 929 (1986).
[45] S. Hikami, Phys. Rev. B **24**, 2671 (1981).
[46] The first term of Eq. (21) coincides with the RMT result [34,35] provided that the discrete ordinate μ_0 is choosen to be equal to $1/2$ that corresponds to the isotropy hypothesis underlying RMT.
[47] R. Berkovits and S. Feng, Phys. Rev. Lett. **65**, 3120 (1990).
[48] R. G. Newton, *Scattering Theory of Waves and Particles* (Dover, New York, 2002).
[49] Formula (25) is in agreement with the result of Ref. [14] where it was shown that the four-point Hikami box within the second order of the gradient (or momentum) expansion does not contain any non-Born contributions.
[50] D. B. Rogozkin and M. Y. Cherkasov, Phys. Rev. B **51**, 12256 (1995).